LETTER

Increasing the critical temperature of Nb films by chemically linking magnetic nanoparticles using organic molecules

To cite this article: Eran Katzir *et al* 2014 *EPL* **108** 37006

A Letters Journal Exploring the Frontiers of Physics

November 2014

EPL, **108** (2014) 37006 www.epljournal.org
doi: 10.1209/0295-5075/108/37006

Increasing the critical temperature of Nb films by chemically linking magnetic nanoparticles using organic molecules

Eran Katzir[1], Shira Yochelis[1], Felix Zeides[2], Nadav Katz[2], Silke Behrens[3], Yoav Kalcheim[2], Oded Millo[2(a)] and Yossi Paltiel[1(b)]

[1] *Applied Physics Department and the Center for Nano-Science and Nano-Technology, the Hebrew University of Jerusalem - Jerusalem, 91904 Israel*
[2] *Racah Institute of Physics and the Center for Nano-Science and Nano-Technology, the Hebrew University of Jerusalem - Jerusalem, 91904 Israel*
[3] *Insitute of Catalysis Research and Technology, Karlsruhe Institute of Technology - Karlsruhe, Germany*

received 28 August 2014; accepted in final form 20 October 2014
published online 10 November 2014

PACS 74.25.Ha – Magnetic properties including vortex structures and related phenomena
PACS 74.25.Wx – Vortex pinning (includes mechanisms and flux creep)

Abstract – In type-II superconductors vortex pinning enhances the critical current density. One known method to induce pinning sites is the use of magnetic nanostructures that locally degrade the superconductivity via stray fields. In recent studies, we showed that both the critical temperature and critical current of Nb thin films can be enhanced by coupling Au nanoparticles via organic molecules and, concomitantly, a zero-bias peak appeared in the density of states. One suggested mechanism to explain these effects was the interaction of the induced pinning potential landscape with the Cooper pairs and vortices. To further examine this mechanism we study in the present work the effects of chemically linking magnetic nanoparticles to Nb films. Two types of magnetic nanoparticles are investigated, half-metal (Fe_3O_4) and metallic (Co). For high nanoparticle density, resulting in an effective continuous magnetic film, the critical temperature is reduced, as expected. However, for intermediate density, where the magnetic nanoparticles are well separated and a distinct pinning landscape is formed above the Nb film, critical temperature and current density enhancements are observed for both types of particles. Moreover, the tunnelling spectra acquired on the (metallic) Co nanoparticles exhibit a zero-bias conducting peak. The magnetic nanoparticles proximity through organic molecules presents similar behaviour to the non-magnetic Au nanoparticles inverse proximity results. This may suggest that pinning mechanisms play a role in the critical temperature enhancement.

Introduction. – In proximity between ferromagnets and singlet-pairing superconductors the order parameter is strongly suppressed in both materials. A standard configuration to overcome this suppression is to introduce an insulating layer between the two systems. Nonetheless, in this configuration the magnetic field induced by the ferromagnet still interacts with the superconductor [1]. In the presence of ferromagnetic nanoparticles (NPs) the stray field generated by the NPs, arranged only few nanometres away from the superconductor's surface, can strongly affect the superconductor by locally degrading the order-parameter and thus introducing local pinning sites [2]. Under an external magnetic field the flux vortices interact with these pinning sites [3,4]. As a result, it can change the transport properties, enhance the superconductor critical current and it is expected to lower the phase transition temperature. Moreover, vortices that are strongly interacting with the magnetic NPs may form coupled magnetic-superconducting topological defects [5].

Previous experimental work on magneto-transport in nanostructured-ferromagnetic/superconductor hybrid systems has focused on the pinning properties induced by stray fields from the ferromagnetic nanostructured arrays coupled to thin superconducting films [6–9]. Several theoretical models were suggested to explain the pinning interactions in such systems. Some suggested that the reduction of the order parameter close to the magnetic nanostructure is a result of the magnetic proximity effect or a consequence of the stray fields [10,11]. In these

(a) E-mail: milode@mail.huji.ac.il (corresponding author)
(b) E-mail: paltiel@cc.huji.ac.il (corresponding author)

experiments the periodicity of the Abrikosov vortex lattice, determined by the magnitude of the external magnetic field, can be fixed to match the periodicity of the ferromagnetic arrays, resulting in a critical current density (J_c) enhancement. It is also well known that pinning properties of the magnetic arrays depend on several factors such as orientation of the magnetic moment, the external magnetic field and the NPs' and superconductors magnetic properties [12]. On the other hand, the effects of magnetic pinning sites on the critical temperature (T_c) are still not clear and remain controversial [13].

In a recent study we found experimentally a unique antiproximity effect, which occurred when gold NPs were chemically linked to a superconducting Nb thin film via organic molecules [14]. The main phenomena observed was a significant T_c enhancement by up to 10% upon NPs adsorption, a dependence on NPs size, length of the organic linker and Nb film thickness. Moreover, scanning tunnelling spectroscopy data acquired on the Au NPs below T_c, exhibited a zero-bias conductance peak (ZBCP). These experimental observations provide new insights into the interaction between superconductivity and nanosized objects, a subject currently drawing substantial theoretical as well as experimental attention [14]. Several mechanisms were suggested to account for the above results, among them are i) increasing the Cooper pairing strength due to Coulomb interaction between the Nb film and the Au NPs [15]; ii) suppression of the surface phonon effect that tends to reduce T_c of the bare film [16]; iii) coupling between the electronic states at the NPs and the superconductor without significant charge transfer, an approach related to Ginsburg model for realizing high-temperature superconductivity [17]; iv) enhancing the pairing-interaction by increased screening the Coulomb repulsion within a two-band model [18]. Lastly, an additional mechanism suggested for the T_c enhancement is related to pinning of vortices at sites caused by the adsorbed Au NPs. Here, one can speculate that at the quasi-2D Nb-molecule interface superconductivity vanishes via a Berezinskii-Kosterlitz-Thouless (BKT) transition [19,20], a transition that may be hindered due to the NP-induced enhanced vortex pinning. One possible way for checking the validity of the latter mechanism is to increase the pinning strength by employing magnetic NPs. Following the above considerations, we turned to study the effect of chemically linked magnetic NPs on the critical temperature of thin Nb films. Here we report an inverse proximity effect, namely, T_c enhancement of the Nb film, upon coupling of both half-metallic and metallic magnetic NPs, Fe_3O_4 (magnetite) and Co, respectively. In that respect, it is interesting to note that weak magnetization was found to emerge in nanosized Au NPs [21] (although smaller than those used in ref. [14]), possibly pointing out a circumstantial link between magnetization and T_c enhancement.

Methods. – Magnetite is known for its strong magnetic properties and for being super-paramagnetic for the sizes and temperatures studied here. The magnetite NPs provided by Sigma-Aldrich are 10 nm in diameter dissolved in toluene. The Co nanoparticles were synthesized under inert conditions by a modified procedure, previously described in ref. [22]. Briefly, 3.235 g (9.5 mmol) $Co_2(CO)_8$ were dissolved in 200 ml toluene, 3.95 mL (17.0 mmol) 3-aminopropyl triethoxy silane were added and the reaction mixture heated to 70 °C (heating rate 6 °C/min). 700 μL (2.0 mmol) N-oleyl sarcosine (KorantinSH, BASF AG) were then injected, before the solution was further heated to 110 °C and stirred for 2 h at this temperature. The solution was concentrated to 40 mL in a rotary evaporator. Additionally, 500 μL N-oleyl sarcosine were added and the mixture heated at 60 °C for further 1.5 h. The Co nanoparticles were obtained as a colloidal solution in toluene and revealed a hydrodynamic diameter of 10 nm as determined by dynamic light scattering experiments. Both types of particles show super-paramagnetic behaviour at room temperature and a blocking temperature around 100 K [23,24].

Our measurements were performed around the Nb critical temperature below 10 K. Scanning tunnelling spectroscopy (STS) measurements on similar magnetite NPs showed an intrinsic gap about 200–300 meV wide developing below the Verwey transition [25,26]. This gap excludes low-energy electronic states from coupling to the Nb film. The magnetic moment of the NPs depends on the cooling process and change between cooling under magnetic field (FC) or zero-field cooling (ZFC) with no external magnetic field [23,24]. Any external magnetic field at lower temperatures will increase the magnetic moment of the NPs resulting with higher stray fields that will increase the pinning force by locally weakening superconductivity.

Nb thin films were sputtered on Si epitaxial ready wafers. The film thickness was approximately 80 nm and the critical temperature of the bare film was around 8.4 K. After characterizing the films properties they were coated with self-assembled organic molecules, 3-methylpropane bis-trichlorosilane (diSilane) provided by Gelest Inc., that form a 3 nm thick layer, as described elsewhere [14]. On top of the organic layer the magnetite NPs were adsorbed. An illustration of the hybrid system can be seen in fig. 1(a) and a scanning electron microscope (SEM) image of the NPs adsorbed on top of the self-assembled organic molecules is shown in fig. 1(b). The density of the NPs depends on the initial NPs concentration in the toluene solution and the adsorption time. Figure 1(b) shows a typical situation of high concentration of magnetite NPs as compared to intermediate coverage presented in the inset of fig. 3(a). In the high-concentration case, the NPs coverage is comprehensive and acting similarly to a full NPs film coverage. The resulting stray fields of the individual NPs are expected to be smoothed out, so the notion of matching field in the conventional form is not expected to apply here. Rather we expect to have an average effect which influences the superconductor's properties, similar to the case of a continuous magnetic film.

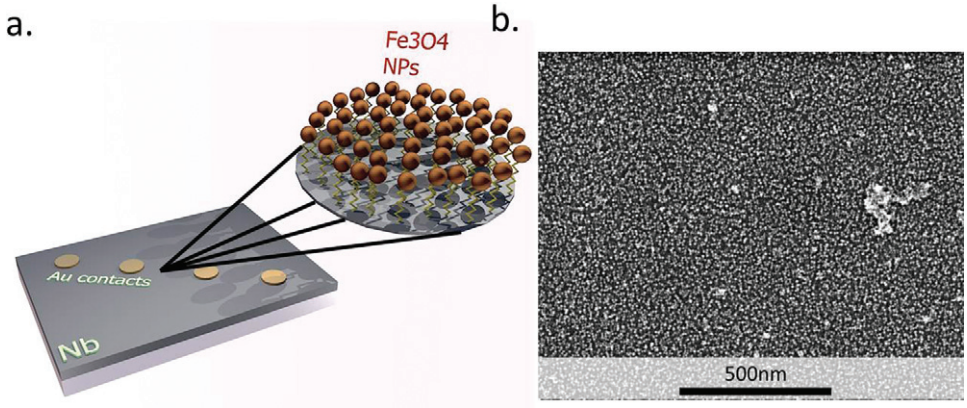

Fig. 1: (Colour on-line) (a) Illustration of the measurement system. (b) Scanning electron microscopy image of the high-density coverage of 10 nm Fe_3O_4 NPs that form a quasi-film of NPs onto the Nb superconductor separated by 3 nm organic monolayer.

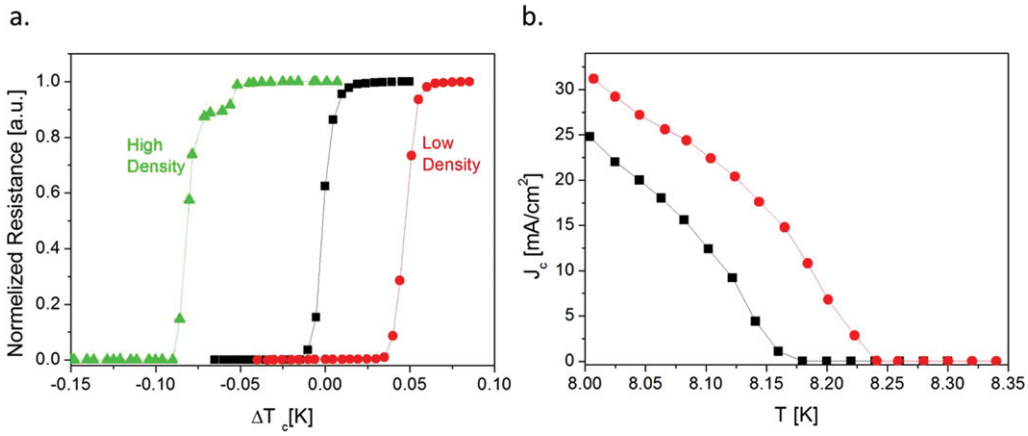

Fig. 2: (Colour on-line) Temperature phase transition of 80 nm Nb superconductor film. (a) Bare film (black/square), magnetite NPs adsorption at intermediate coverage (red/circle) and high magnetite NPs coverage (green/triangle). The high density corresponds to 1% reduction and the low density to 0.7% enhancement in T_c compared to the bare sample of 8.17 K. The ΔT_c is related to the peak in the derivative of the bare sample resistance. (b) Critical current density of the Nb film as a function of temperature before (black/square) and after (red/circle) intermediate density of magnetite NPs adsorbtion. The voltage threshold chosen was 1 μV at 0 T external magnetic field.

The scanning tunneling microscopy and spectroscopy (STM and STS) measurements were performed at 4.2 K using a Pt-Ir tip. Several measurements were performed at temperatures above 10 K to verify that the spectroscopic features associated with superconductivity (gaps and ZBCPs) vanished above the critical superconducting temperature of the Nb film. Topographic images were taken in the standard constant current mode with bias voltages of ∼100 mV, well above the superconducting gap voltage of Nb. The tunneling conductance $\mathrm{d}I/\mathrm{d}V$ *vs.* V spectra (proportional to the local density of states), were numerically derived from the current-voltage (I-V) curves measured while momentarily disconnecting the STM feedback loop.

Results and discussion. – All samples were zero-field-cooled to cryogenic temperatures before measurements. Transport measurements were taken using a four probe configuration scheme (see fig. 1(a)), where each data point was averaged over 20 sequential measurements to reduce the noise. All bare samples studied here showed nearly the same critical temperature, T_c of 8.2–8.4 K, varied by their quality and defects. However, in our experiment we compare between the same sample, with the same contacts, before (bare) and after (nanoparticles adsorption), in the same initial conditions. For each sample the T_c measurement was repeated 10 times producing a critical temperature value with standard deviation of 2.5 mK. Figure 2(a) depicts resistance-*vs.*-temperature curves measured on the pristine Nb film (black curve) and after linking magnetite NPs at intermediate and high densities (red and green curves, respectively). All three datasets exhibit a sharp superconducting transition, allowing a clear identification of the T_c modifications upon NP adsorption. In the intermediate coverage case we clearly observe T_c enhancement by about 0.05 K (much larger than

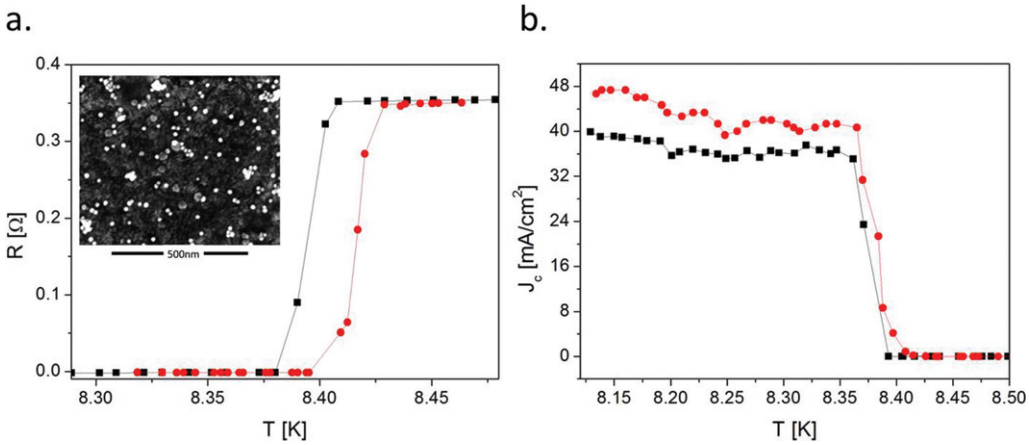

Fig. 3: (Colour on-line) Resistance as a function of temperature for the bare sample (black/square) and after (red/circle) Co NPs adsorption. (a) T_c enhancement is clearly observed. In the inset: SEM image of a typical intermediate NPs adsorption, in this case Co NPs. Critical current density enhancement is observed after Co NPs adsorption (b).

the transition width). An opposite behaviour was found in the high-coverage case, where T_c reduced typically by 0.1 K, a result conforming to the expected proximity effect. The stray field created due to the high-density coverage of NPs is expected to exhibit moderate spatial vitiations, over typical length scales larger than the coherence length in Nb, $\xi \sim 40$ nm. Therefore, the pinning landscape, and in particular the local pinning sites, will be smoothened out. In contrast, at intermediate density of NPs, where the NPs are separated from one another by a distance comparable to ξ, strong and localized pinning sites are expected to reside near the individual NPs. The strong pinning potential is expected to enhance J_c. Figure 2(b) portrays critical current measurements before and after the adsorption of intermadate density NPs, and indeed a clear increase in J_c is seen.

It is important to note that a self-assembled organic monolayers, without the NPs, were reported to reduce the critical current of Nb due to a field effect that diminishes the pinning force [14,27]. Only by adding the magnetic nanoparticles improvement in the crtical temperature can be achieved.

In previous experiments [14] enhancement of T_c due to linking of Au NPs was accompanied by an appearance of a ZBCP in the tunneling spectra measured on the NPs. The ZBCP can be associated with vortex traping in a pinning site, since in the vortex core the density of electron (quasiparticle) states may increase due to the formation of Andreev bound states [28]. In the present experiment, however, the intrinsic gap (of about 200–300 meV) developing in the magnetite below the Verwey temperature (∼120 K) masks the ZBCP if it exists, as well as any other possible induced superconducting features.

This latter problem does not hold for the metallic Co NPs we studied for comparison (see below), which have similar super-paramagnetic properties as the half-metal magnetite NPs. We linked the Co NPs to the

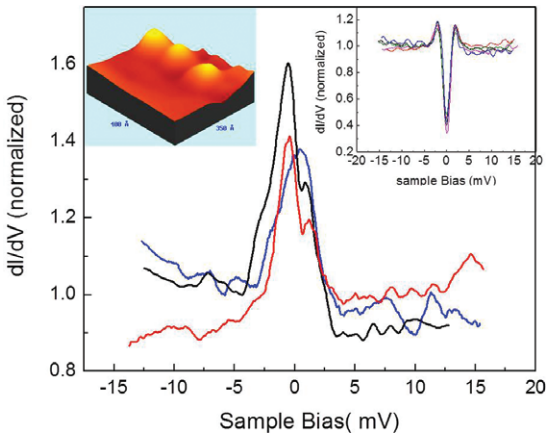

Fig. 4: (Colour on-line) Tunneling spectra acquired at 4.2 K on top of three Co NPs, appeared in a row (see the topographic image in the left inset). All NPs show zero-bias peak. The right inset shows the supercondcutor's gap in an area without NPs. The topographic image size is 40 × 35 nm.

superconductor using the same diSilane organic molecules. Figure 3 shows that also in this case T_c and J_c increase after the Co NPs adsorption. Note that the critical current enhancement is very similar for the two types of magnetic NPs, indicating that the magnetic pinning mechanism and strength are the same in both cases.

Further possible evidence for vortex pinning is provided by the STS data presented in fig. 4, which depicts dI/dV-*vs.*-V tunneling spectra acquired at 4.2 K ($< T_c$) for three different Co NPs adsorbed on the Nb film (shown in the left inset). These spectra, which reflect the local quasiparticle density of states, show a clear peak at zero bias that was absent above T_c and appeared only on the NPs. Aside from the NPs, the tunneling spectra revealed the superconducting gap of Nb, somewhat smeared probaly due to the presence of the molecules (right inset). It is well known that Andreev bound states may develop at

the vortex core, and in some cases also at zero energy, and these may appear in the tunneling spectra as a ZBCP [29]. Although the nature of the ZBCPs observed in our case is not entirely clear, in particular because it appears to be soemwhat wider than anticipated, it may emerge from a vortex core trapped in a pinning site formed by the stray field of the NP, and possible life-time broadened due to the magnetic NP [30].

We now turn to address the possible contribution of vortex pinning to the T_c enhancement shown in figs. 2 and 3, and in ref. [14]. Such a scenario is possible assuming that in the quasi–two-dimensional Nb-molecule interface superconductivity disappears via a Berezinskii-Kosterlitz-Thouless (BKT) transition [19,20], where it is destroyed by phase fluctuations due to the unbinding of thermally excited vortex-antivortex pairs. This process can be hindered due to vortex pinning, resulting in increased T_c. Early predictions attribute the T_c enhancement to renormalization of the inter-vortex interaction [31]. These show that in the presence of small disorder the BKT transition temperature should increase, and a decrease in critical temperature is expected with large disorder. The fact that nearly the same T_c enhancement was found for the two types of magnetic NPs studied here, having very different electronic properties, suggests that out of the mechanisms proposed above for the enhancement, the one related to vortex pinning may play an imprtant role. This conjecture gains support from the fact that the critical current increase was also very similar for the two types of NPs. Recall that J_c is directly related to the pinning force determined by the magnetic moments of the NPs that are indeed similar. The magnetic interaction is expected to degrade the superconductivity of the Nb film. Therefore, the fact that *any* enhancement was observed also upon attaching magnetic NPs is even more surprising than our previous observation for Au NPs. The enhancement in the latter system [14] was considerably higher for both films with lower and larger thickness. We note in passing that it is not surprising that the enhancement in the latter system was considerably higher. One expects the proximity effect and corresponding T_c reduction to be much smaller in conventional (planar) superconductor/Au interfaces compared to superconductor/ferromagnet interfaces. Consequently, the final outcome which results from these two competing processes, proximity and pinning, is weaker for the magnetic system.

In addition, mechanisms associated with some kind of charge or quasiparticle transfer, which could further assist in T_c enhancement, are expected to be more effective for the Au NPs compared to their insulating Fe_3O_4 counterparts.

Summary. – In the present work we investigate the coupling of magnetic NPs of two types, half-metal (Fe_3O_4) and metallic (Co), to Nb superconductor thin film. We were able to measure enhancement of both the critical temperature and critical current for intermediate coverage of NPs, where the NPs are separated from one another by a distance comparable to ξ, the coherence length in Nb. The fact that the T_c increase was very similar for the two types of NPs, having very different electronic properties yet similar vortex-pinning attributes, suggests that vortex pinning plays a significant role also in this unique effect. STS measurements that were taken on the Co NP showed ZBCPs, which could be associated with a bound state at the vortex cores trapped in pinning sites created by the magnetic nanoparticles.

* * *

OM and YP would like to acknowledge the Leverhulme trust IN-2013-033, NK and FZ acknowledge ISF grant No. 1248/10 for financial support and the HUJI center for nano science and nano technology for their assistance in sample preparation and characterization.

REFERENCES

[1] Lange M., Bael M. J. V., Bruynseraede Y. and Moshchalkov V. V., *Phys. Rev. Lett.*, **90** (2003) 197006.
[2] Priour D. J. and Fertig H. A., *Phys. Rev. Lett.*, **93** (2004) 057003.
[3] Gomez A., Gilbert D. A., Gonzalez E. M., Liu K. and Vicent J. L., *Appl. Phys. Lett.*, **102** (2013) 052601.
[4] Palau A., Parvaneh H., Stelmashenko N. A., Wang H., Macmanus-Driscoll J. L. and Blamire M. G., *Phys. Rev. Lett.*, **98** (2007) 117003.
[5] Lyuksyutov I. F. and Pokrovsky V. L., *Adv. Phys.*, **54** (2005) 67.
[6] Vélez M., Martín J. I., Villegas J. E., Hoffmann A., González E. M., Vicent J. L. and Schuller I. K., *J. Magn. & Magn. Mater.*, **320** (2008) 2547.
[7] Otani Y., Pannetier B., Nozières J. P. and Givord D., *J. Magn. & Magn. Mater.*, **126** (1993) 622.
[8] Martín J. I., Vélez M., Hoffmann A., Schuller I. K. and Vicent J. L., *Phys. Rev. B*, **62** (2000) 9110.
[9] Jaccard Y., Martín J. I., Cyrille M.-C., Vélez M., Vicent J. L. and Schuller I. K., *Phys. Rev. B*, **58** (1998) 8232.
[10] Lyuksyutov I. F. and Pokrovsky V., *Phys. Rev. Lett.*, **81** (1998) 2344.
[11] Erdin S., Kayali A. F., Lyuksyutov I. F. and Pokrovsky V. L., *Phys. Rev. B*, **66** (2002) 014414.
[12] Van Bael M. J., Van Look L., Temst K., Lange M., Bekaert J., May U., Güntherodt G., Moshchalkov V. V. and Bruynseraede Y., *Physica C: Supercond.*, **332** (2000) 12.
[13] Chen L., Tsai C.-F., Zhu Y., Bi Z. and Wang H., *Physica C: Supercond.*, **471** (2011) 515.
[14] Katzir E., Yochelis S., Zeides F., Katz N., Kalcheim Y., Millo O., Leitus G., Myasodeyov Y., Shapiro B. Y., Naaman R. and Paltiel Y., *Phys. Rev. Lett.*, **108** (2012) 107004.
[15] Leggett A. J., *J. Supercond. Nov. Magn.*, **19** (2006) 187.
[16] Noffsinger J. and Cohen M. L., *Phys. Rev. B*, **81** (2010) 214519.

[17] Ginzburg V. L., *Sov. Phys. Usp.*, **19** (1976) 174.
[18] Entin-Wohlman O. and Imry Y., *Phys. Rev. B*, **40** (1989) 6731.
[19] Kosterlitz J. M. and Thouless D. J., *J. Phys. C: Solid State Phys.*, **6** (1973) 1181.
[20] Berezinskiĭ V. L., *JETP*, **32** (1971) 493.
[21] Guerrero E., Muñoz-Márquez M. A., García M. A., Crespo P., Fernández-Pinel E., Hernando A. and Fernández A., *Nanotechnology*, **19** (2008) 175701.
[22] Gorschinski A., Khelashvili G., Schild D., Habicht W., Brand R., Ghafari M., Bönnemann H., Dinjus E. and Behrens S., *J. Mater. Chem.*, **19** (2009) 8829.
[23] Yang H. T., Shen C. M., Su Y. K., Yang T. Z., Gao H. J. and Wang Y. G., *Appl. Phys. Lett.*, **82** (2003) 4729.
[24] Goya G. F., Berquó T. S., Fonseca F. C. and Morales M. P., *J. Appl. Phys.*, **94** (2003) 3520.
[25] Maris G., Shklyarevskii O., Jdira L., Hermsen J. G. H. and Speller S., *Surf. Sci.*, **600** (2006) 5084.
[26] Poddar P., Fried T., Markovich G., Sharoni A., Katz D., Wizansky T. and Millo O., *Europhys. Lett.*, **64** (2003) 98.
[27] Shvarts D., Hazani M., Shapiro B. Y., Leitus G., Sidorov V. and Naaman R., *Europhys. Lett.*, **72** (2005) 465.
[28] Aprili M., Covington M., Paraoanu E., Niedermeier B. and Greene L. H., *Phys. Rev. B*, **57** (1998) R8139.
[29] Hess H. F., Robinson R. B., Dynes R. C., Valles J. M. and Waszczak J. V., *Phys. Rev. Lett.*, **62** (1989) 214.
[30] Dynes R. C., Narayanamurti V. and Garno J. P., *Phys. Rev. Lett.*, **41** (1978) 1509.
[31] José J. V., *Physica B+C*, **107** (1981) 493.